Nature of the process of overdriven shocks in metals

Duane C. Wallace
Los Alamos Scientific Laboratory, Los Alamos, New Mexico 87545
(Received 6 February 1981)

Within the bounds established by the formal theory of overdriven shocks in solids, an approximate solution is constructed, and a consistent set of approximations for the thermodynamic coefficients is described. Numerical calculations of the temperature, entropy, shear stress, and plastic strain, as functions of compression, are shown for shocks up to 0.8 Mbar in 2024 Al, and up to 3.0 Mbar in Pt. For well-overdriven shocks in metals the shock entropy is generated by heat conduction in the front part of the shock, the heat is generated by plastic flow in the last part of the shock, and the shock rise time is of order 10^{-12} s.

I. INTRODUCTION

We have obtained extensive theoretical information about the irreversible-thermodynamic process of overdriven shocks in solids.[1] This theory was developed for an isotropic solid with heat transport and dissipative plastic flow, and a steady-wave shock which does not induce phase changes or macroscopic inhomogeneities in the solid. The purpose of the present work is to carry out numerical calculations to see what can be learned about the details of the shock process, without assuming anything about the plastic flow behavior. Calculations are done for 2024 Al for shocks of 0.4 and 0.8 Mbar, and for Pt for shocks of 0.5 — 3.0 Mbar. Information is obtained on temperature, entropy, shear stress, plastic strain, and heat current, as functions of compression, and the space and time dependence of the process is estimated.

All the approximations used in the numerical evaluations are described in Sec. II, and their physical bases and implications are discussed. Results are tabulated and discussed in Sec. III, and the salient features of overdriven shocks in metals are summarized in Sec. IV. The status of an investigation into the validity of irreversible thermodynamics in shock theory is mentioned in Sec. IV. For the two metals studied here, properties on the Hugoniot are tabulated in the appendixes.

II. AN APPROXIMATE SOLUTION

A. The conduction front

In general, except for shocks not far above the overdriven threshold, the shock process is narrowly bounded by the theory of Ref. 1. The bounds for the temperature $T(\epsilon)$ for a 2.5 Mbar shock in Pt are shown by the solid lines in Fig. 1. Our aim is to construct an approximate $T(\epsilon)$ curve within these bounds, thus defining a partial solution, and then to solve as far as possible the Rayleigh-line equations for the other functions of this partial solution, the entropy per unit mass $S(\epsilon)$, the heat

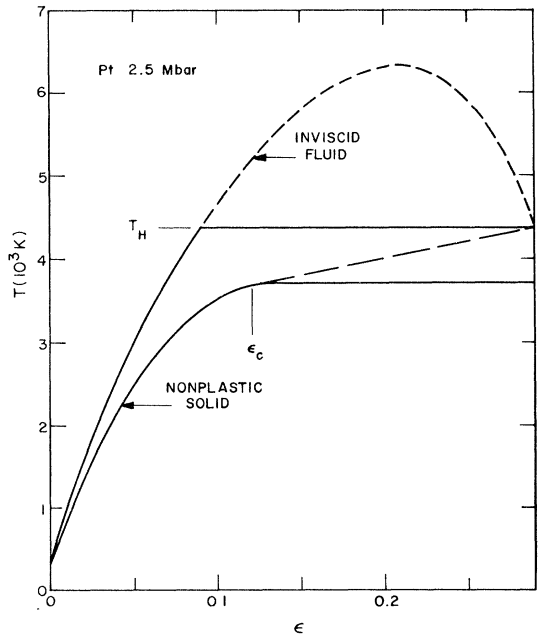

FIG. 1. Solid lines show upper and lower bounds for $T(\epsilon)$ for a 2.5 Mbar shock in Pt. Our approximate solution takes the lower bound (nonplastic solid curve) up to point c, and the linear interpolation (dashed line) from $T_c(\epsilon_c)$ to $T_H(\epsilon_H)$.

current $J(\epsilon)$, the plastic strain $\psi(\epsilon)$, and the shear stress $\tau(\epsilon)$.

At the beginning of the shock, in state a, τ and $\dot{\psi}$ are zero. As the uniaxial compression begins, τ increases due to elastic response of the material but $\dot{\psi}$ remains zero unitl τ reaches the static yield value. When τ increases above the static yield, plastic flow proceeds. However, since the shock process is quite fast, its timescale being governed by heat conduction, the plastic flow will be of negligible importance until τ rises high enough to drive ψ at a very high rate, a rate commensurate with the shock rise time. Thus in the leading part of the shock we should have $d\psi=0$ to a good approximation, i.e., we have nearly the response of an elastic solid with infinite yield strength, as described in Theorem 3.[1] We take this approximation to hold up to a point c, at ϵ_c, to be determined later. The region $0\leq\epsilon\leq\epsilon_c$ is called the conduction front because heat must be transported to this region, according to Theorem 1.[1] The Rayleigh-line equations for the conduction front as function of ϵ are Eqs. (32) — (35) of Ref. 1. These equations are accurately represented by their leading terms in the small-anisotropy expansion, and this representation is used in the present calculations.

B. The flow region

After the point c the plastic flow gets going at a high rate, and the temperature rises significantly above the nonplastic solid curve. From ϵ_c to ϵ_H, $T(\epsilon)$ goes from the nonplastic solid curve to T_H, increasing monotonically with ϵ, as illustrated by the dashed line in Fig. 1. The region $\epsilon_c\leq\epsilon\leq\epsilon_H$ is called the flow region, because here the dissipative plastic flow is essential to the process. Before approximating $T(\epsilon)$ in the flow region, we will study the Rayleigh-line equations here in some detail.

In the flow region, it is necessary to keep both dissipative mechanisms in the equations. First consider the equation for $d\tau$; in the small-anisotropy expansion this is written

$$d\tau=-G(d\ln V+\tfrac{3}{2}d\psi)+\cdots\ . \tag{1}$$

The leading terms in $d\tau$ are thus of order $Gd\epsilon$. There are a host of first-order terms, indicated by $+\cdots$ in (1), of relative order τ/G, which means of order $(\tau/G)Gd\epsilon$ in $d\tau$. These terms involve the third-order elastic constants, the anisotropic Gruneisen parameters, and so on. From Eq. (1) we learn two things:

(a) Since $d\tau$ is of order $\tau d\epsilon$, the leading terms must cancel to relative order τ/G, which implies

$$d\psi\approx-\tfrac{2}{3}d\ln V\ . \tag{2}$$

(b) $d\tau$ depends *essentially* on the first-order terms in (1).

In practice it is not possible to make respectable estimates of *all* the coefficients appearing in the first-order terms in $d\tau$ along the Rayleigh line for overdriven shocks in solids. If we cannot estimate all the coefficients in the first-order terms in $d\tau$, we cannot make a meaningful evaluation of $d\tau$ in the flow region. We conclude that we cannot use Eq. (1) in the flow region.

There are three equations which couple the normal stress $\sigma(\epsilon)$, and $T(\epsilon)$, $S(\epsilon)$, $\psi(\epsilon)$ on the Rayleigh line, namely Eqs. (5), (9), and (11) of Ref. 1. When $\sigma(\epsilon)$ is eliminated, the results can be written as two equations for $S(\epsilon)$ and $\psi(\epsilon)$ in terms of $T(\epsilon)$. Neither of these equations depends critically on the terms of relative order τ/G; meaningful evaluations of both are obtained in zeroth order in the small-anisotropy expansion. In this order the equations are the following:

$$TdS=C_V(dT-\rho\gamma V_a T d\epsilon)\ , \tag{3}$$

$$d\psi=(2G)^{-1}\{\rho\gamma T dS - [\rho_a D^2-\rho V_a(B+\tfrac{4}{3}G)]d\epsilon\}\ . \tag{4}$$

Thus if we have an acceptable approximation for $T(\epsilon)$ in the flow region, (3) can be integrated to find $S(\epsilon)$, then (4) can be integrated to find $\psi(\epsilon)$. The coefficients in (3) and (4) can be evaluated with respectable accuracy on the Rayleigh line for real metals.

Finally there is the equation for the entropy production,[1]

$$TdS=dJ/\rho_a D+2V\tau d\psi\ . \tag{5}$$

This cannot be solved because it contains two unknowns, J and τ. However, because of the initial and final conditions $J_a=J_H=0$, we have an integral condition on dJ, namely $\int_a^H dJ=0$. Hence $\int_a^H T\,dS=\int_a^H 2V\tau\,d\psi$, and this is $\int_c^H 2V\tau\,d\psi$ because $d\psi=0$ on $0\leq\epsilon\leq\epsilon_c$. This last integral is used to define a mean shear stress $\langle\tau\rangle$ in the flow region:

$$\int_c^H 2V\tau\,d\psi=(V_c+V_H)\langle\tau\rangle\int_c^H d\psi\ . \tag{6}$$

Then $\langle\tau\rangle$ can be evaluated from

$$\langle\tau\rangle=\frac{\int_a^H TdS}{(V_c+V_H)\psi_H} . \tag{7}$$

To emphasize an important point, this estimate of $\langle\tau\rangle$ is not based on Eq. (1) for $d\tau$, which is essentially a first-order equation and hence is extremely difficult to evaluate, but is based on an integral condition for TdS, namely the requirement that the shear stress must do the correct amount of work in the flow region to generate the correct amount of heat, so the material reaches the correct Hugoniot state at the end of the shock. A reasonably accurate evaluation of $\langle\tau\rangle$ can be made for real metals.

The above results for $S(\epsilon)$ and $\psi(\epsilon)$ in the flow region and for $\langle\tau\rangle$ do not depend strongly on the curve of $T(\epsilon)$ in the flow region. We take simply a straight line interpolation for $T(\epsilon)$ from $T_c(\epsilon_c)$ to $T_H(\epsilon_H)$, and define c as the point on the nonplastic solid $T(\epsilon)$ curve which is tangent to the straight line drawn from $T_H(\epsilon_H)$. This approximation is shown for a 2.5 Mbar shock in Pt by the dashed line in Fig. 1. There is a technical point which should be mentioned: The approximation for $T(\epsilon)$ in the flow region should be consistent with the physical requirement that $d\psi/d\epsilon$ be non-negative. Now $dJ/d\epsilon=0$ at ϵ_b, and for the nonplastic solid partial solution both terms on the right side of (4) are zero at ϵ_b, and ϵ_c is close to ϵ_b so $d\psi/d\epsilon$ is always small at ϵ_c, but it can be negative. In the numerical calculations of the present work, $d\psi/d\epsilon$ is found to be essentially zero at ϵ_c.

C. The Hugoniot

We are studying shocks upwards from a few hundred kbar, where nothing is known of the shear stress on the Hugoniot. While the shear stress during the shock becomes large, driving plastic flow at a high rate, all strain rates go to zero at the end of the shock, and the final-state shear stress is the static yield stress on the Hugoniot. For overdriven shocks in metals τ_H/σ_H should be at most a few percent, so neglecting τ_H should not introduce a significant error in the present calculations. We therefore set $\tau_H=0$, which reduces σ_H to an isotropic pressure P_H.

The Hugoniot jump conditions are the first integrals of the equations for conservation of mass, momentum, and energy, evaluated at the final state H [see, e.g., Ref. 1, Eqs. (3) – (5)].

Since our approximate Hugoniot lies in isotropic thermodynamic space, the thermoelastic coefficients on the Hugoniot are reduced to isotropic coefficients, e.g., $\gamma_1=\gamma_2=\gamma$, where

$$\rho\gamma=\left[\frac{\partial P}{\partial U}\right]_V . \tag{8}$$

Equations for calculating T and S on the Hugoniot and the adiabatic bulk modulus on and off the Hugoniot are well known.[2] A well-established experimental result for shocks in solids up to a few Mbar, and excepting cases where phase changes occur, is that the shock velocity is a linear function of the final-state particle velocity[2–4]:

$$D=c+sv_H . \tag{9}$$

The constant c and s are commonly measured for overdriven shocks in solids.

D. Thermodynamic coefficients

In the small-anisotropy expansions,[1] anisotropic coefficients on the anisotropic Rayleigh line at V,S,τ are given in lowest order by isotropic coefficients at V,S; for example,

$$C_\eta(V,S,\tau)=C_V(V,S)+\cdots . \tag{10a}$$

This relation is to be understood when we say "C_V on the Rayleigh line." In the present work we will need γ, C_V, B, and G on the Rayleigh line. Further, because the relation between T and S is evaluated to lowest order in the small anisotropy expansion, which is Eq. (3), the T,V,S relation on the Rayleigh line is in fact the isotropic-space T,V,S relation, so (10a) can also be written

$$C_\eta(V,T,\tau)=C_V(V,T)+\cdots . \tag{10b}$$

For the Grüneisen parameter we use the approximation[5] $\rho\gamma=$ const:

$$\rho\gamma=\rho_a\gamma_a . \tag{11}$$

The heat capacity is the sum of a lattice part C_l and an electronic part C_e. The lattice part is described in terms of a characteristic temperature Θ, e.g., the Debye temperature, where for most metals Θ is less than or equal to room temperature at $P=0$. If $T_a\gtrsim\Theta$, then the Hugoniot and Rayleigh lines all lie in the region $T\gtrsim\Theta$, where $C_l\approx 3Nk$, with $k=$ Boltzmann's constant. For the conduction electrons, degenerate electron theory gives $C_e=\Gamma T$. We will neglect the explicit temperature-dependence of Γ,[6] and use low-temperature measurements for Γ.[7] The volume-

dependence is[8] $g=d\ln\Gamma/d\ln V\approx 1-2$, and we take $g=$ const for a given metal. The total heat capacity is then approximately

$$C_V=3Nk+\Gamma T\ , \tag{12a}$$

$$\Gamma=\Gamma_a(V/V_a)^g\ . \tag{12b}$$

The shear modulus is entirely unknown in the moderate shock region. The common behavior of polycrystalline materials at $P=0$ is $G/B\approx$ constant in T, except near melting. We will assume this holds for shocks in the solid phase, and calculate G on the Rayleigh line from B,

$$G/B=G_a/B_a\ . \tag{13}$$

As a point of curiosity we calculated B and G for Al from ultrasonic data,[9] in the form of expansions linear in T and P from state a, and found the remarkable results that B(ultrasonic) $\approx B$(shock), and G/B(ultrasonic) $\approx$ const, up to 2 Mbar (neglecting melting) on the Hugoniot. These calculations are tabulated in Appendix B.

The thermal conductivity κ is needed only to compute the explicit space and time dependence of the shock process, from the equation[1]

$$dZ=\frac{-\kappa dT}{(1-\epsilon)J}\ , \tag{14}$$

where $Z=X-Dt$. For electronic conduction in the region $T/\Theta\gtrsim 1$, we expect κ to be nearly independent of T, and to have a density dependence of order ρ to ρ^2.[1] This density dependence is negligible for the present purposes, and we simply take $\kappa=$ constant and use the measured value of κ at $T/\Theta\gtrsim 1$, $P=0$.

E. Shock thickness and plastic strain rate

The Lagrangian shock thickness ΔZ, the same as ΔX at a fixed time, is usually defined in terms of the compression $\epsilon(Z)$ (Ref 10); we call this the compression thickness $\Delta Z(\epsilon)$:

$$\frac{\Delta\epsilon}{\Delta Z(\epsilon)}=\left|\frac{d\epsilon}{dZ}\right|_{\max}\ . \tag{15}$$

The temperature profile $T(Z)$ is noticeably broader than the compression, so we define also the temperature thickness $\Delta Z(T)$:

$$\frac{\Delta T}{\Delta Z(T)}=\left|\frac{dT}{dZ}\right|_{\max}\ . \tag{16}$$

Either derivative $|d\epsilon/dZ|$ or $|dT/dZ|$ is near its maximum at point c, and this gives a simple approximation for the right sides of (15) and (16). For example,

$$\Delta Z(T)\approx\frac{\kappa(T_H-T_a)}{(1-\epsilon_c)J_c}\ .$$

The Lagrangian rise time is then $\Delta t_X=\Delta Z/D$.

The plastic strain rate $\dot{\psi}$ is approximated as follows: $d\psi$ is given by (4), dJ is approximated in the flow region by (5) with $2V\tau d\psi\approx(V_c+V_H)\langle\tau\rangle d\psi$, then dZ is given by (14), and

$$\dot{\psi}=\left[\frac{\partial\psi}{\partial t}\right]_X-D\frac{d\psi}{dZ}\ . \tag{17}$$

A useful measure of plastic strain rate in the shock is the average of $\dot{\psi}$ in the flow region, defined by

$$\langle\dot{\psi}\rangle=\frac{\int_c^H\dot{\psi}\,d\epsilon}{\epsilon_H-\epsilon_c}\ . \tag{18}$$

F. On the electronic contributions

There are several important points to note regarding the electronic contribution to thermodynamic coefficients.

(a) For shocks in the Mbar range, electronic contributions to thermal energy and thermal pressure are not always negligible and should at least be estimated. This was pointed out by Al'tshuler.[11]

(b) In shock analysis, if the electronic heat capacity $C_e=\Gamma T$ cannot be neglected, then the volume dependence of Γ also cannot be neglected because of the significant compression. Including $C_e=\Gamma T$ with a constant value of Γ seriously overestimates C_e.

(c) The Grüneisen parameter γ is not simply the sum of a lattice part γ_l and an electronic part γ_e (Ref. 6, p. 287). Specifically, Eq. (8) can be transformed to $\rho\gamma=-C_V^{-1}(\partial^2F/\partial V\partial T)_{TV}$, where F is the Helmholtz free energy, the sum of a lattice and an electronic part, $F=F_l+F_e$, from which it follows:

$$\gamma=(C_l/C_V)\gamma_l+(C_e/C_V)\gamma_e\ .$$

It is γ we want for shock analysis, to calculate *total* P,U relations from Eq. (8), and it is γ which satisfies $\rho\gamma\approx$ const in Neal's[5] compilation.

(d) Degenerate electron theory is satisfactory for kT/ϵ_F is less than or equal to a few tenths, where ϵ_F is the Fermi energy. For sufficiently strong shocks, which may be above the melting tempera-

ture on the Hugoniot, the temperature will rise so high that the electrons are no longer degenerate.

III. RESULTS AND DISCUSSION

The experimental information for the present shock calculations for 2024 Al and Pt is listed in Table I. The Hugoniot was calculated first, and results are tabulated in Appendix A. Several observations follow from the Hugoniot calculations.

(a) The elastic precursor velocity c_p is very close to the longitudinal sound velocity c_l, so the overdriven threshold at $D=c_p$ is close to $D=c_l$; we find

$$P_H(D=c_l)=0.145 \text{ Mbar for 2024 Al}, \quad P_H(D=c_l)=0.308 \text{ Mbar for Pt}. \tag{19}$$

(b) From the Kraut-Kennedy melting rule,[13] melting on the Hugoniot is found to occur at

$$T_M=2715 \text{ K}, \quad P_M=0.88 \text{ Mbar for 2024 Al}, \quad T_M=5800 \text{ K}, \quad P_M=3.04 \text{ Mbar for Pt}. \tag{20}$$

To the extent this approximation is in error, we expect it to be low for T_M, P_M.

(c) Neglecting the electronic heat capacity gives a calculated temperature on the Hugoniot too high by about 4% at 0.9 Mbar for 2024 Al, and too high by about 33% at 3 Mbar for Pt. For details see Appendix A.

The approximate solution for the shock process was computed for 2024 Al for shocks of 0.4 and 0.8 Mbar, and for Pt for six shocks of strength 0.5 — 3.0 Mbar. The main results are listed in Table II. The shape of the shock process as a function of the compression ϵ, and as a function of shock strength, is shown by the Pt sequence in Figs. 2—4. Note that as the shock strength increases, the width ϵ_c of the conduction front becomes larger compared to the width ϵ_H of the entire shock. In the weakly overdriven shock at 0.5 Mbar, only about a quarter of the shock temperature rise T_H-T_a occurs in the conduction front, and the entropy continues to increase in the flow region. In the well-overdriven shocks, 1 Mbar and stronger, at least three quarters of the shock temperature rise occurs in the conduction front, and the entropy decreases in the flow region. The results for 2024 Al show the same qualtitative behavior. We conclude that for well-overdriven shocks, in the present calcultions at shock pressure around three times the overdriven threshold or greater, heat conduction is a major part of the process, and most of the shock temperature rise occurs in the conduction front. For weaker shocks the effect of heat conduction becomes smaller as the shock strength decreases toward the overdriven threshold. In fact since the initial compression of the solid is presumably elastic, in the small ϵ region $J(\epsilon)\to 0$ as $D\to c_l$, and for $D\leq c_l$ a solution can be obtained without heat transport. We consider the effect of heat transport to be generally negligible for underdriven shocks in solids.[14]

Because of the shape of $T(\epsilon)$ on the Rayleigh line, it appears that for shocks near melting on the Hugoniot, but still in the solid phase there, $T(\epsilon)$ will rise above the equilibrium melting temperature for a time in the center of the shock. When T passes the melting temperature, the material should begin to respond as a fluid after a time of order t_s, the shear relaxation time of the fluid phase. For most monatomic fluids, $t_s\sim 10^{-13}$ s at zero pressure, and should decrease roughly as $(V/V_a)^\gamma$ in compression. However, fluid behavior depends on the presence of vacancies, and during the shock there may not be time to develop the equilibrium concentration of vacancies, since this is presumably a diffusion process. The time required for fluid response to occur during a shock is an interesting open question.

As mentioned before, our approximate solution for $T(\epsilon)$ is reasonably accurate because of the narrow bounds imposed by the formal theory[1] (see, e.g., Fig. 1; also Fig. 4 of Ref. 1). In the flow region, these bounds limit $T(\epsilon)$ to within a deviation from the mean of $\pm 20\%$ for the two weakest shocks in Table II, namely 0.4 Mbar for 2024 Al

TABLE I. Input data for shock calculations. Shock measurements (c,s) are from McQueen *et al.* (Ref. 2) for 2024 Al and from Morgan (Ref. 12) for Pt; G_a/B_a are from the poly- crystal averages of Simmons and Wang (Ref. 9); and g are from White and Collins (Ref. 8).

Quantity	2024 Al	Pt
T_a (10^3 K)	0.293	0.293
ρ_a (g/cm^3)	2.785	21.44
c (cm/μs)	0.533	0.363
s	1.338	1.472
γ_a	2.05	2.66
G_a/B_a	0.34	0.23
Γ_a (10^{-4} cal/mole K^2)	3.30	16.4
g	1.8	2.28
κ (cal/cm s K)	0.48	0.20

TABLE II. Results of the shock process calculations.

Quantity	2024 Al		Pt					
P_H (Mbar)	0.4	0.8	0.5	1.0	1.5	2.0	2.5	3.0
ϵ_H	0.2363	0.3241	0.1200	0.1863	0.2311	0.2642	0.2903	0.3114
D (cm/μs)	0.779	0.941	0.441	0.500	0.550	0.594	0.634	0.670
T_H (10^3 K)	0.930	2.365	0.534	1.132	2.032	3.138	4.374	5.697
$S_H - S_a$ (cal/mole K)	4.10	8.83	1.84	5.79	9.29	12.1	14.5	16.5
ϵ_c	0.0565	0.1130	0.0155	0.0544	0.0825	0.1044	0.1210	0.1355
$J_c/\rho_a D$ (10^3 cal/mole)	1.81	8.17	0.34	3.61	8.77	15.0	21.9	29.2
T_c (10^3 K)	0.648	1.903	0.359	0.919	1.755	2.699	3.685	4.680
$S_c - S_a$ (cal/mole K)	4.15	10.19	1.06	6.79	11.23	14.5	17.1	19.3
τ_c (Mbar)	0.019	0.048	0.011	0.044	0.075	0.107	0.136	0.167
ψ_H	0.162	0.226	0.081	0.126	0.158	0.182	0.202	0.219
$\langle\tau\rangle$ (Mbar)	0.027	0.064	0.021	0.053	0.086	0.121	0.16	0.19
$\langle\dot{\psi}\rangle$ (10^{12}/s)	0.06	0.27	0.011	0.12	0.32	0.43	0.48	0.51
$\Delta Z(\epsilon)$ (10^{-6} cm)	1.30	0.48	2.47	0.32	0.18	0.17	0.18	0.19
$\Delta Z(T)$ (10^{-6} cm)	2.23	1.41	2.90	0.90	0.71	0.65	0.61	0.58

and 0.5 Mbar for Pt, and to within a deviation of $\pm 10\%$ for the other shocks. The $T(\epsilon)$ bounds can be transformed to bounds on $\tau(\epsilon)$, from the variational relation[1]

$$\delta\tau(\epsilon) = -\tfrac{3}{4}\rho\gamma C_V \delta T(\epsilon) .$$

From this we estimate that our computed values of $\langle\tau\rangle$ have error bounds of $\pm 23\%$ for the two weakest shocks in Table II, and of $\pm 10-15\%$ for the other shocks.

The space-time dependence of the Pt 2.5 Mbar shock is shown in Fig. 5, where $Z=0$ is at point c in the shock. The difference in behavior of the temperature and entropy, as compared with the compression, is clearly seen: Because of the massive long-range transport of heat in the conduction front, the profiles of T and S extend far ahead of point c, and the increases of T and S are large

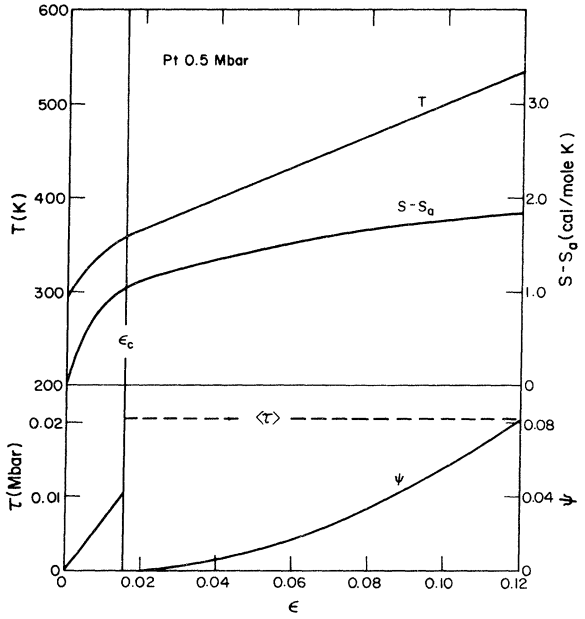

FIG. 2. Shape of the shock process for a 0.5 Mbar shock in Pt.

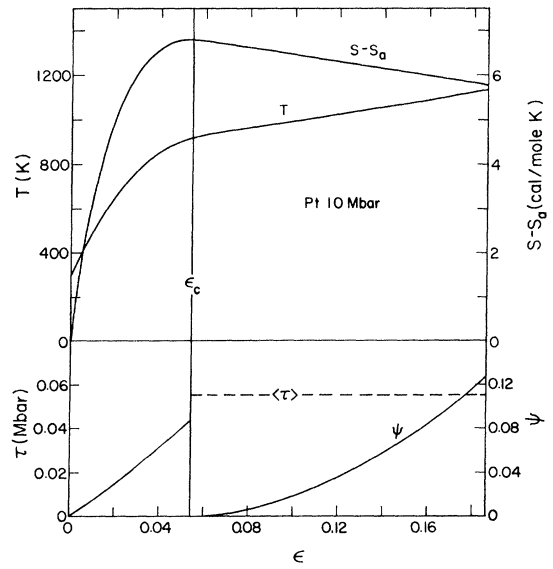

FIG. 3. Shape of the shock process for a 1.0 Mbar shock in Pt.

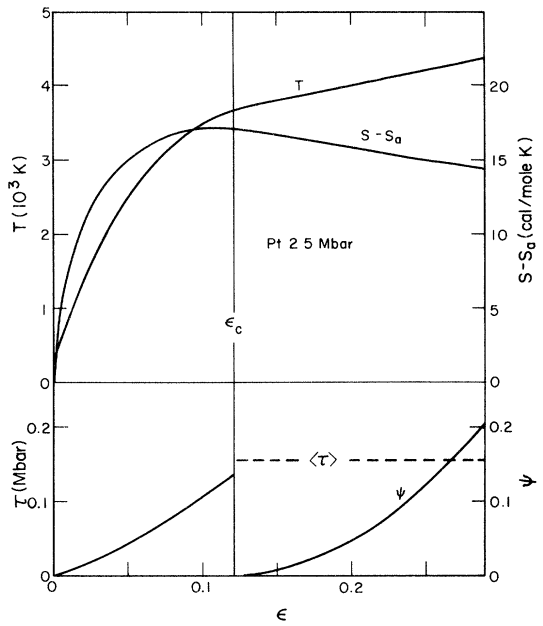

FIG. 4. Shape of the shock process for a 2.5 Mbar shock in Pt.

there; then behind point c, T and S change little while most of the compression takes place. Note, however, that in the limits $Z\to\pm\infty$, all three functions T,S,ϵ have formally the same Z dependence. In particular, for $Z\to\infty$, $T-T_a$, $S-S_a$, and ϵ all approach zero as $e^{-\alpha Z}$, with α a constant; and for $Z\to-\infty$, $|T-T_H|$, $|S-S_H|$, and $|\epsilon-\epsilon_H|$ all approach zero as $e^{\beta Z}$, with β another constant. In the same way, $\psi\to\psi_H$ and $\dot{\psi}\to 0$ behind the shock.

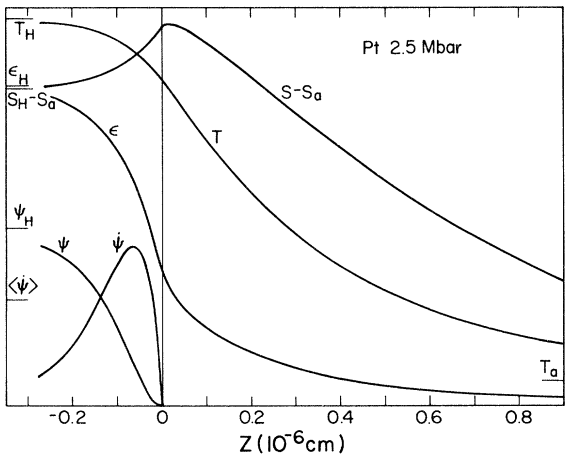

FIG. 5. Shock process as function of Z for a 2.5 Mbar shock in Pt.

Concerning the plastic constitutive behavior through the shock process, we note that $\langle\tau\rangle$ is larger than τ_c for all the shocks. This is consistent with setting $\dot{\psi}=0$ up to point c. In a real solution, of course, plastic flow will start at a much lower value of τ than τ_c, but $\dot{\psi}$ should still be small in the conduction front, and should increase significantly around point c, so the qualitative behavior of ψ and $\dot{\psi}$ should be still as shown in Figs. 2–5. Since the total ψ is small in a planar shock, strain hardening should be correspondingly small, and the high shear stress we find in the flow region is presumably due to the high strain rate $\dot{\psi}$. Finally, while we expect our estimates of $\langle\tau\rangle$ and $\psi(\epsilon)$ to be reasonably accurate, it is difficult to establish bounds for $\psi(\epsilon)$, and only order-of-magnitude meaning can be claimed for our values of $\langle\dot{\psi}\rangle$. For all but the weakest Pt shock in Table II, the ratio $\langle\tau\rangle/\langle\dot{\psi}\rangle$ lies in the range 0.2–0.4 g/cm s.

IV. NATURE OF THE SHOCK PROCESS

We review the nature of shocks in solids, for different ranges of shock strength. Recall that the elastic line is the $\sigma(\epsilon)$ relation corresponding to isentropic uniaxial elastic compression of the solid (see, e.g., Fig. 1 of Ref. 1). In a weak (underdriven) shock, the initial compression is on the elastic line; this signal travels as the elastic precursor. Following this initial elastic compression, the normal stress σ falls *below* the elastic line; hence a solution can be obtained by allowing plastic flow to occur, to relax σ below the elastic line.[14] The effect of heat transport on the shock process is presumably negligible. Since the elastic precursor travels faster than the plastic wave, the entire shock is not a steady wave.

For an overdriven shock, we *assume* the shock is a steady wave. The normal stress rises above the elastic line at small ϵ, so heat transport is necessary to obtain a solution in the leading edge. As the shock strength increases from the overdriven threshold, the quantity of heat which must be transported to the conduction front increases from zero. Also in the vicinity of the overdriven threshold, as shock strength increases, there is a dramatic decrease in the shock rise time, a decrease of a factor of order 10^3 for metals.

As a qualitative definition, a well-overdriven

TABLE III. Hugoniot for 2024 A1. Units are the following: P (Mbar), T (K), S (cal/mole K).

ϵ	P	T	$S-S_a$	T_{ion}
0	0	293	0	293
0.04	0.035	319	0.018	319
0.08	0.079	354	0.157	354
0.12	0.135	411	0.56	411
0.16	0.205	507	1.35	509
0.20	0.295	675	2.59	679
0.24	0.412	962	4.27	974
0.28	0.566	1446	6.30	1474
0.30	0.662	1799	7.41	1842
0.32	0.774	2252	8.58	2319
0.34	0.905	2835	9.79	2938
0.36	1.060	3583	11.04	3741

shock is one in which most of the shock temperature rise occurs in the conduction front. For well-overdriven shocks in solids, the theory we have developed is characterized by the following properties:

(a) Essentially all of the shock entropy is generated in the conduction front, by heat conduction.

(b) The heat is generated in the flow region, by plastic flow.

(c) For metals the shock thickness is $\Delta Z \sim 10^{-6}$ cm, the risetime is $\Delta t \sim 10^{-12}$ s.

(d) For shocks near melting on the Hugoniot, but still in the solid phase there, $T(\epsilon)$ rises above the equilibrium melting temperature for a time in the center of the shock.

Once the detailed space and time dependence of the shock process is found, it is possible to examine conditions on the validity of irreversible thermodynamics, in terms of the relaxation times and the mean free paths of electrons and phonons. The preliminary conclusion from this study, for steady-wave shocks in solid or liquid metals, is that the present theory is a valid approximation for shocks up to a definite limit and is invalid for all stronger shocks. The breakdown of irreversible thermodynamics results from the massive demand for heat transport and the consequent inability of electrons and phonons to remain near equilibrium. The limit is in the range of a few Mbar for metals.

TABLE IV. Hugoniot for Pt. Units are the following: P (Mbar), T (K), S (cal/mole K).

ϵ	P	T	$S-S_a$	T_{ion}
0	0	293	0	293
0.04	0.128	329	0.067	329
0.08	0.290	395	0.56	398
0.12	0.500	534	1.84	546
0.16	0.773	816	4.00	859
0.20	1.135	1348	6.81	1478
0.24	1.621	2283	10.03	2646
0.26	1.928	2967	11.7	3557
0.28	2.289	3839	13.5	4782
0.30	2.718	4942	15.4	6427
0.32	3.231	6327	17.3	8630

TABLE V. Elastic moduli calculated on the Hugoniot for A1, neglecting melting. Units are the following: P (Mbar), T (K), B (Mbar), G (Mbar).

P_H	T_H-T_a	B_H	B_u/B_H	G_u/B_u
0	0	0.79	0.96	0.345
0.2	207	1.55	1.04	0.37
0.4	637	2.20	1.10	0.37
0.6	1274	2.80	1.15	0.37
0.8	2072	3.37	1.18	0.36
1.2	4015	4.47	1.21	0.35
1.6	6270	5.54	1.23	0.34
2.0	8730	6.58	1.25	0.33

ACKNOWLEDGMENTS

The author appreciates helpful discussions with R. G. McQueen, B. R. Suydam, and R. A. Axford.

APPENDIX A: THE HUGONIOT

Thermodynamic functions on the Hugoniot for 2024 Al and for Pt are listed in Tables III and IV, respectively. The effect of neglecting the electronic contribution to C_V is shown by the column T_{ion}, which is computed by taking for C_V only the ion vibrational part, $3Nk$ per mole.

APPENDIX B: ELASTIC MODULI ON THE HUGONIOT

A linear expansion of B from state a ($P=0$, $T=T_a$) is

$$B=B_a+(\partial B/\partial P)_T P+(\partial B/\partial T)_P(T-T_a)\,,$$

where the coefficients are to be evaluated at state a.

A similar equation may be written for G. Evaluations of these equations from ultrasonic data are denoted B_u, G_u. For single crystal Al, Thomas[15] measured variations in ultrasonic transit times due to variations in anisotropic stresses up to ~ 25 bar, variations in P up to ~ 50 bar, and variations in T of ~ 10 K. Polycrystalline averages[9] of Thomas's results give

$$B_u = 0.759 + 4.42P - 0.16(10^{-3})(T - T_a) ,$$

$$G_u = 0.262 + 1.82P - 0.14(10^{-3})(T - T_a) ,$$

in Mbar, with P in Mbar, T in K, and $T_a = 293$.

The bulk modulus computed on the Hugoniot from shock data is denoted B_H. We ignore melting and the presence of the liquid phase, and we also ignore the difference between pure Al and 2024 Al in order to compare the ultrasonic and shock results, Table V. It is seen that $B_u \approx B_H$ and $G_u/B_u \approx$ const to 2 Mbar on the Hugoniot.

[1]D. C. Wallace, preceding paper, Phys. Rev. B 24, 5597 (1981).

[2]R. G. McQueen, S. P. Marsh, J. W. Taylor, J. N. Fritz, and W. J. Carter, in *High-Velocity Impact Phenomena,* edited by R. Kinslow (Academic, New York, 1970), p. 293.

[3]L. V. Al'tshuler, N. N. Kalitkin, L. V. Kuz'mina, and B. S. Chekin, Zh. Eksp. Teor. Fiz. 72, 317 (1977) [Sov. Phys.—JETP 45, 167 (1977)].

[4]W. M. Isbell, F. H. Shipman, and A. H. Jones, Report No. MSL-68-13 (General Motors, Warren, Michigan).

[5]T. Neal, Phys. Rev. B 14, 5172 (1976).

[6]D. C. Wallace, *Thermodynamics of Crystals* (Wiley, New York, 1972).

[7]C. Kittel, *Thermal Physics* (Wiley, New York, 1969).

[8]G. K. White and J. G. Collins, J. Low-Temp. Phys. 7, 43 (1972); G. K. White, J. Phys. F 2, L30 (1972).

[9]G. Simmons and H. Wang, *Single Crystal Elastic Constants and Calculated Aggregate Properties* (MIT, Cambridge, Mass., 1971).

[10]Ya. B. Zel'dovich and Yu. P. Raizer, *Physics of Shock Waves and High-Temperature Hydrodynamic Phenomena* (Academic, New York, 1966), Vol. 1, p. 82.

[11]L. V. Al'tshuler, Usp. Fiz. Nauk 85, 197 (1965) [Sov. Phys.—Uspekhi 8, 52 (1965)].

[12]J. A. Morgan, High Temp. High Pressures 6, 195 (1974).

[13]E. A. Kraut and G. C. Kennedy, Phys. Rev. 151, 668 (1966).

[14]D. C. Wallace, Phys. Rev. 22, 1477, 1487 (1980).

[15]J. F. Thomas, Jr., Phys. Rev. 175, 955 (1968).